65830

USE OF A SPACECRAFT BORNE ALTIMETER FOR DETERMINING THE MEAN SEA SURFACE AND THE GEOPOTENTIAL

W. D. KAHN

J. W. BRYAN

(NASA-TM-X-65830)   USE OF A SPACECRAFT
BORNE ALTIMETER FOR DETERMINING THE MEAN
SEA SURFACE AND THE GEOPOTENTIAL   W.D.
Kahn, et al (NASA)   Jan. 1972   30 p
CSCL 14B

N72-18458

G3/14   19786

—— GODDARD SPACE FLIGHT CENTER ——
GREENBELT. MARYLAND

(ACCESSION NUMBER) 30	(THRU) G3
(PAGES) TMX 65830	(CODE) 14
(NASA CR OR TMX OR AD NUMBER)	(CATEGORY)

FACILITY FORM 602

31 P

USE OF A SPACECRAFT BORNE ALTIMETER FOR DETERMINING THE MEAN SEA SURFACE AND THE GEOPOTENTIAL

W. D. Kahn
J. W. Bryan

January 1972

CONTENTS

USE OF A SPACECRAFT BORNE ALTIMETER FOR DETERMINING THE MEAN SEA SURFACE AND THE GEOPOTENTIAL

by

W. D. Kahn
J. W. Bryan

INTRODUCTION

An experiment is proposed to test a first generation spacecraft-borne radar altimeter's capability to measure the topography of the sea surface. The topography of the sea surface is of interest to geodesy and oceanography. It is of interest to geodesy because the mean sea level surface reflects the structure of the geopotential. That is, since 70% of the earth's surface is covered by oceans, an experimental determination of sea level will lead to a measure of the overall geopotential. The topography of the sea surface is of interest to oceanography because it is a manifestation of the dynamics of ocean circulation and the various forces that shape the ocean surface such as tidal forces, wind stress, and storm surges.

The initial radar altimeter will have an instrumental error of one meter and an overall accuracy of two to five meters (Reference 1). This instrument will thus improve the accuracy of the geoid from the present 10 to 20 meters to better than 5 meters. In order to detect storm surges, tidal forces, ocean currents, an altimeter with an overall accuracy of at least ±1 meter will be required. The overall accuracy of the initial radar altimeter will thus primarily provide geodetic information and possibly oceanographic information such as sea state.

I. OBJECTIVE

An experiment is proposed to utilize a spacecraft borne radar altimeter to detect variations in the ocean heights to about ±2 to ±5 meters. From the analysis of data obtained by an altimeter capable of the aforementioned resolution of surface features, detection of geoidal anomalies having wavelengths of say 200 km (200, 200) field to 2000 km (20, 20) field should be possible. These anomalies cannot now be detected from conventional satellite geodesy, nor may fields higher than (20, 20) ever be obtained via straight satellite ground tracking.

1

A direct consequence from the detection of these short wavelength terms in the geopotential over the global sea surface, will be an improvement to the global geoid accuracy from the present 10 to 20 meters to better than 5 meters.

In order to detect geoidal undulations in the two to five meter range, the altimeter measurements are to be compared with altitude computed from the spacecraft orbit. The altitude calculated from the orbit must therefore be determined to an accuracy of better than ±1 meter in a specific area. Through the use of satellite to satellite tracking combined with precision tracking from ground based tracking systems such as lasers, C-band radars, and Doppler systems for orbit determination, the desired accuracy in S/C height calculated from the orbit should be attainable.

II. SIGNIFICANCE

A. Scientific & Technological

Scientific achievements which can be attained with a radar altimeter lie in its applications for geodesy and oceanography. A satellite-borne radar altimeter represents an initial effort to obtain the topography of the sea surface from a satellite. The major advantage afforded by such an orbiting instrument is its ability to provide extensive global coverage over a relatively short time period. This instrument can through its global coverage provide useful information concerning the shape of the geoid. That is, every square degree of ocean surface will be surveyed 16 times per year by a spacecraft borne altimeter in a near circular orbit having a mean altitude of about 1000 km and an inclination of 65°.

Since the undulation in geoidal height is on the order of 100 meters and the relief of the ocean surface is on the order of ±10 meters with respect to mean sea level, acceptance of ocean topography as geopotential will provide a map of geoidal undulations more accurate than the present accuracy of ±10 to 20 meters associated with the global geoid (Reference 1).

The mapping of the earth's gravity field is now accomplished by two tried and tested methods both having their respective advantage. In one method for global coverage, geopotential information is derived from satellite orbit perturbation techniques. Because the effects of higher harmonic variations of the gravity field fall off rapidly with distance from the earth (Figure 1), short period variations in the geopotential have small amplitudes and hence cannot be sensed.
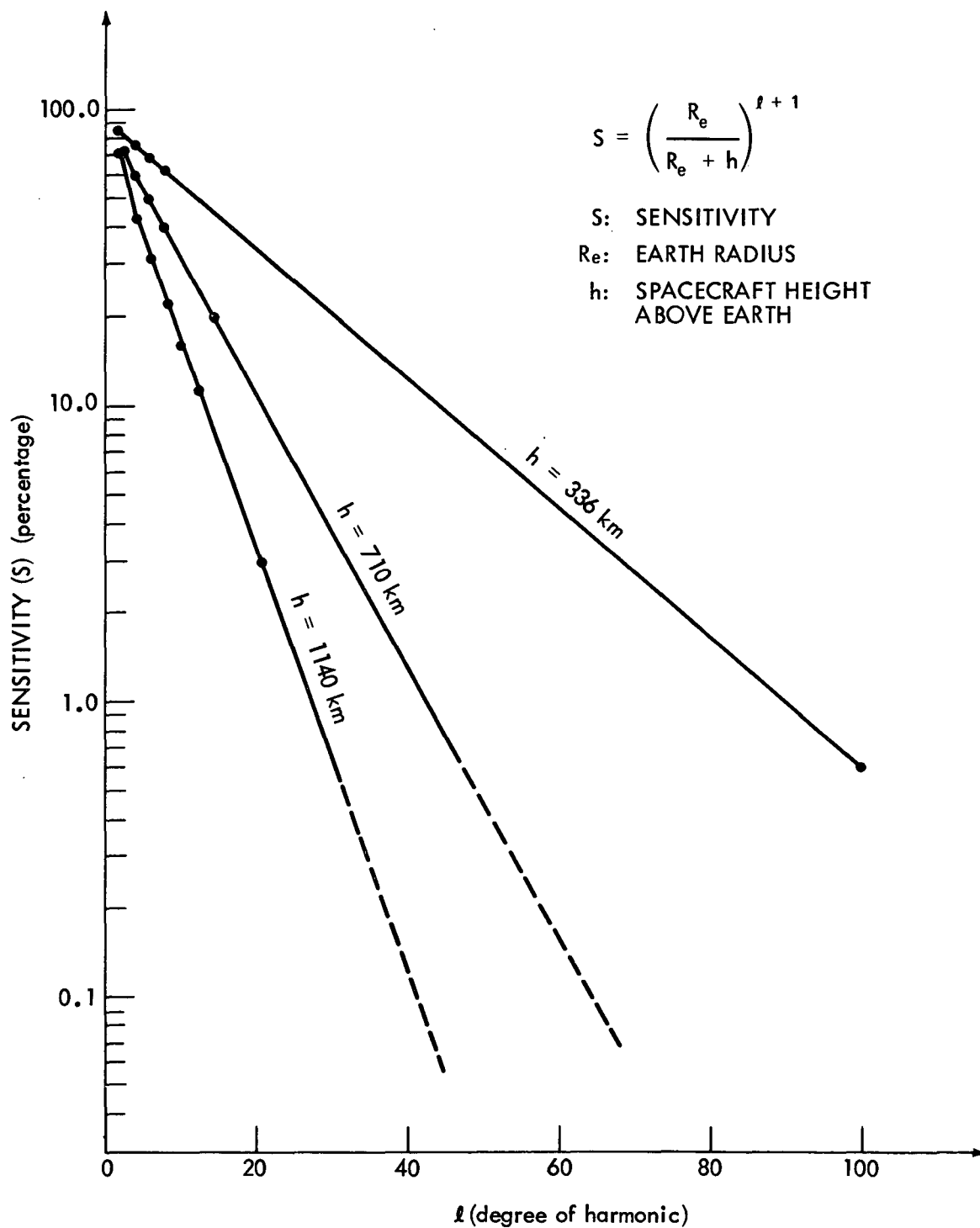
Figure 1. Sensitivity to Spherical Harmonic Terms in Geopotential
as a Function of Spacecraft Height

$$S = \left(\frac{R_e}{R_e + h} \right)^{\ell + 1}$$

S: SENSITIVITY

R_e: EARTH RADIUS

h: SPACECRAFT HEIGHT
ABOVE EARTH

3

The other method which consists of direct measurements of gravity magnitude provides data for sensing short period variations in the geopotential (or sensitive to higher degree and order harmonics). There are, however, large gaps in gravimetric data coverage i.e., only 50% of the global sea surface has been covered (Figure 2). Current practice is to interpolate to fill the gaps, obtain an approximate solution and then combine this in a statistical data fit along with satellite determinations.

For illustrative purposes, a geoidal map of the Caribbean area based on only a satellite derived geopotential (Figure 3) is compared with a geoidal map based on the combination of the satellite geopotential and mean gravity anomalies (Figure 4). In the region of the Puerto Rical Trench lat. 19°N to 21.5°N, longitude 63.5°W to 68°W in Figure 3, a variation of 1 meter in geoidal height can be seen. In Figure 4 a variation of 5 meters in geoidal height can be seen. Based on measurements (made in 1966) of the Geoid in the Puerto Rican Trench area by Von Arx (Reference 5) of the Woods Hole Oceanographic Institution (WHOI) it was found that the geoid changed more than 20 meters over the 2° change in latitude (∼ 220 km). He measured geoidal undulations both astrogeodetically and gravimetrically while the WHOI research vessel, CHAIN, sailed a north to south course. Von Arx' measurements (Figure 5) show the geoid dips down to almost 17 meters below the ellipsoid at 20°N latitude, and then rises to the level of the ellipsoid at 21°N latitude.

Through the combination of surface gravity measurements with the dynamically determined geopotential (Figure 4), short wavelength terms in the geopotential were detected (in this case on the order of 200 km). That is, a 5 meter change in geoidal height out of a maximum change of 17 meters was detected. The detection of a similar change in geoidal height with only the dynamically determined geopotential was not and could not be detected since detection of short wavelengths of the order of 200 km would require an expansion of the geopotential in terms of spherical harmonics through order and degree 90. The SAO standard earth 1969 geopotential is a field of order and degree 16 which means that it is sensitive to wavelengths on the order of 1200 km and greater and tends to smooth over this shorter wavelength.

The initial spacecraft-borne radar altimeter with a capability of resolving surface features in the height-range of 2 to 5 meters should detect variations in geoidal height on the order of those detected by Von Arx over the Puerto Rican Trench. As a consequence of surveying the variation in geoidal height over the global sea surface with the altimeter, an improvement of the geoidal accuracy from the present 10 to 20 meters to 5 meters should be achieved.
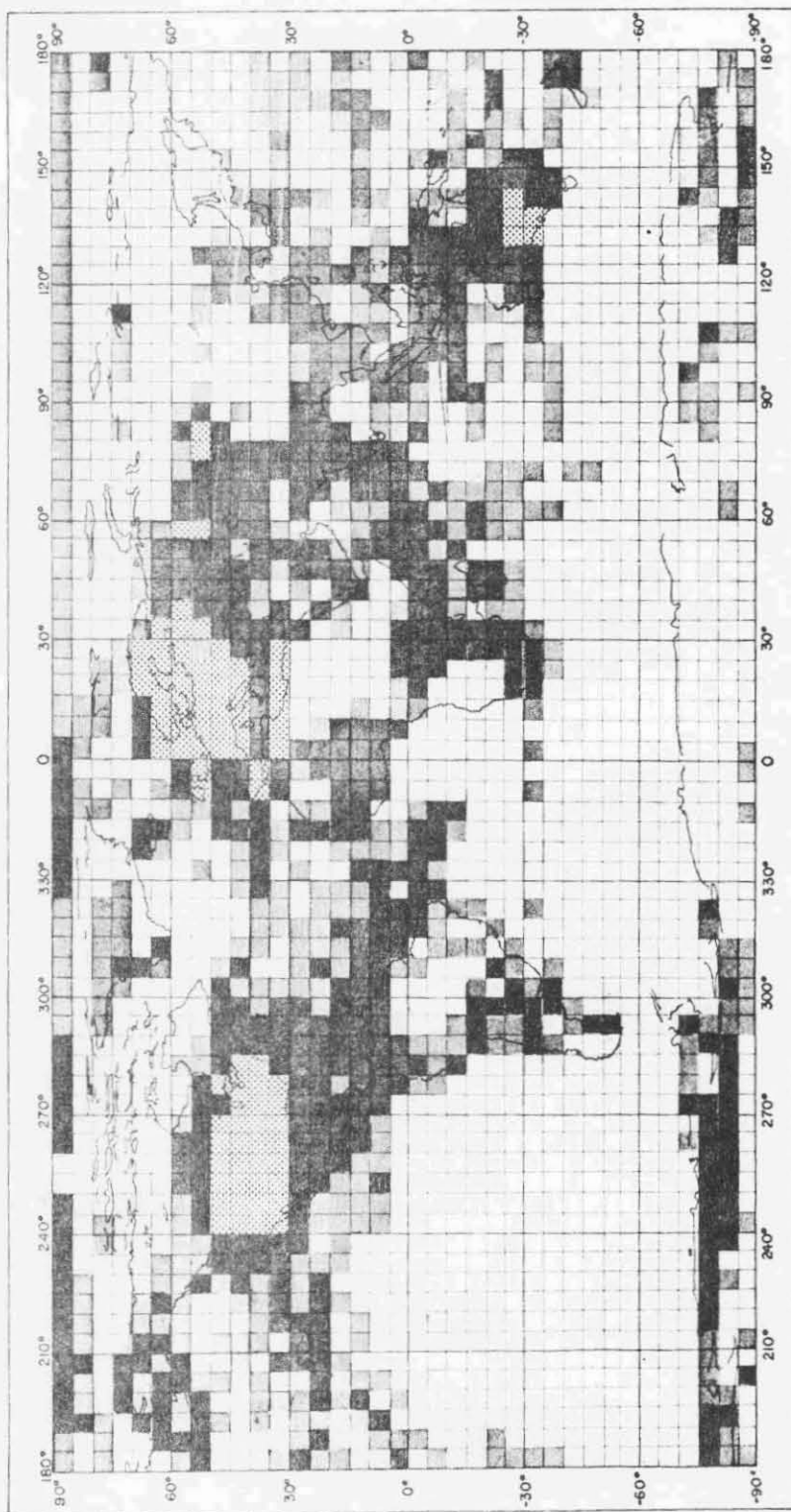
Figure 2.   Distribution and quality of terrestrial gravity data.*

*Rapp, R. H. Gravitational potential of the earth determined from a combination of satellite, observed, and model anomalies. J. Geo-
phys. Res., 73, pp. 6555-6562, 1968.

5

Figure 3. Geoid Based on SAO 1969 Standard Earth
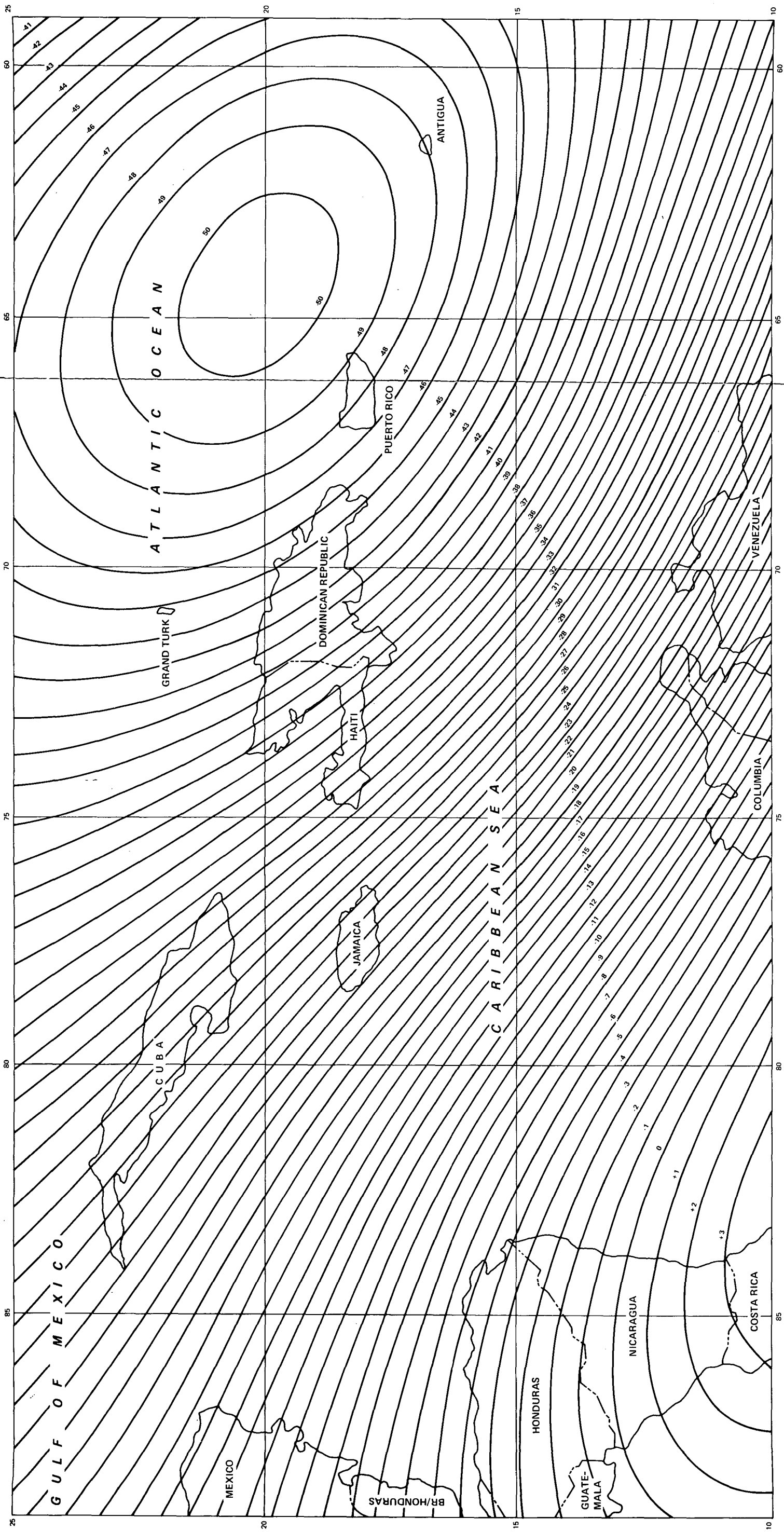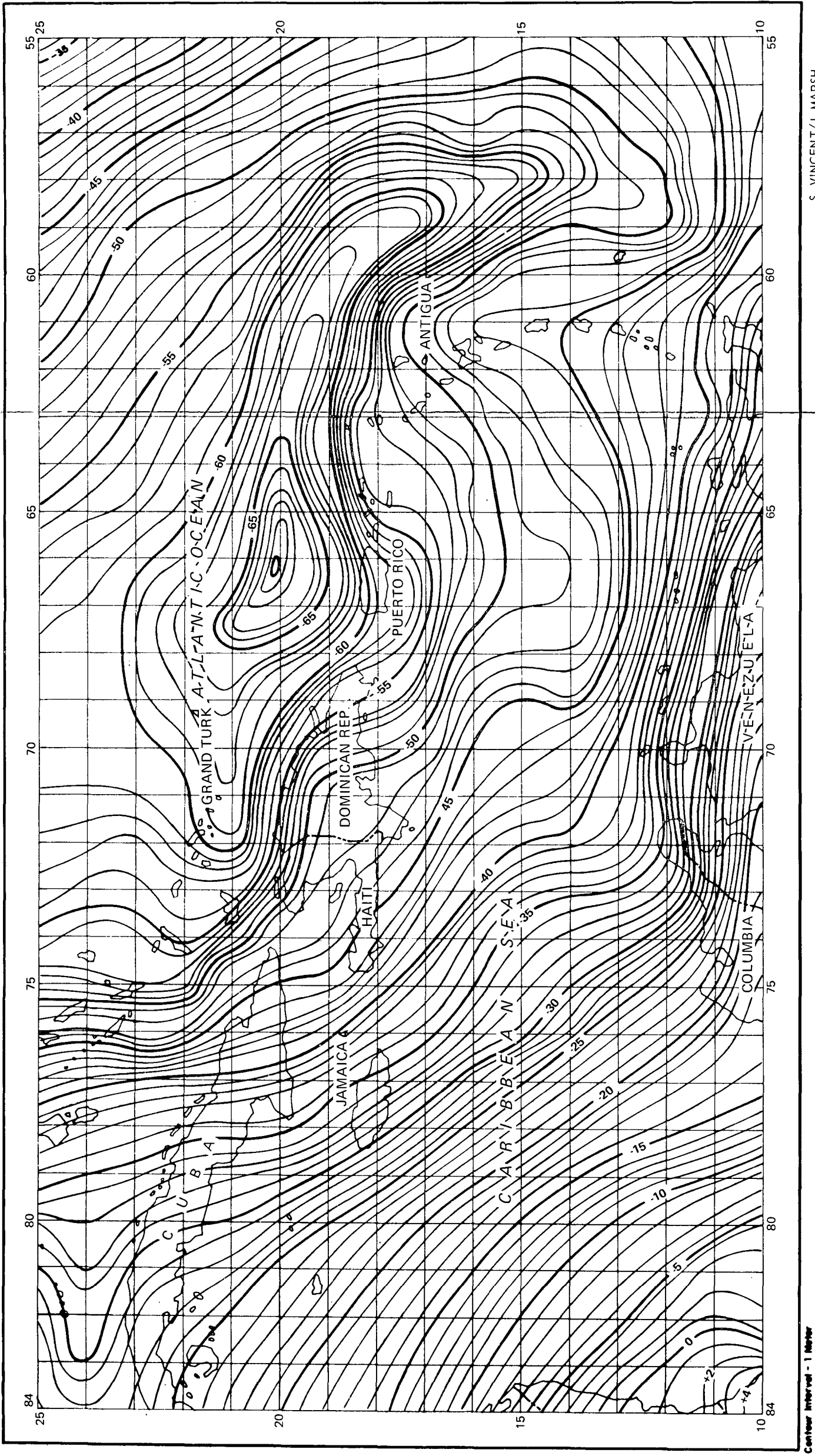
S. VINCENT/J. MARSH
NASA/GSFC 1971 (REFERENCE 4)

7

Figure 4. Detailed Gravimetric Geoid of the Caribbean Using SAO 1969 Standard Earth & Mean Gravity Anomalies for 1° x 1° Squares

Contour Interval - 1 Meter

9

PRECEDING PAGE BLANK NOT FILMED
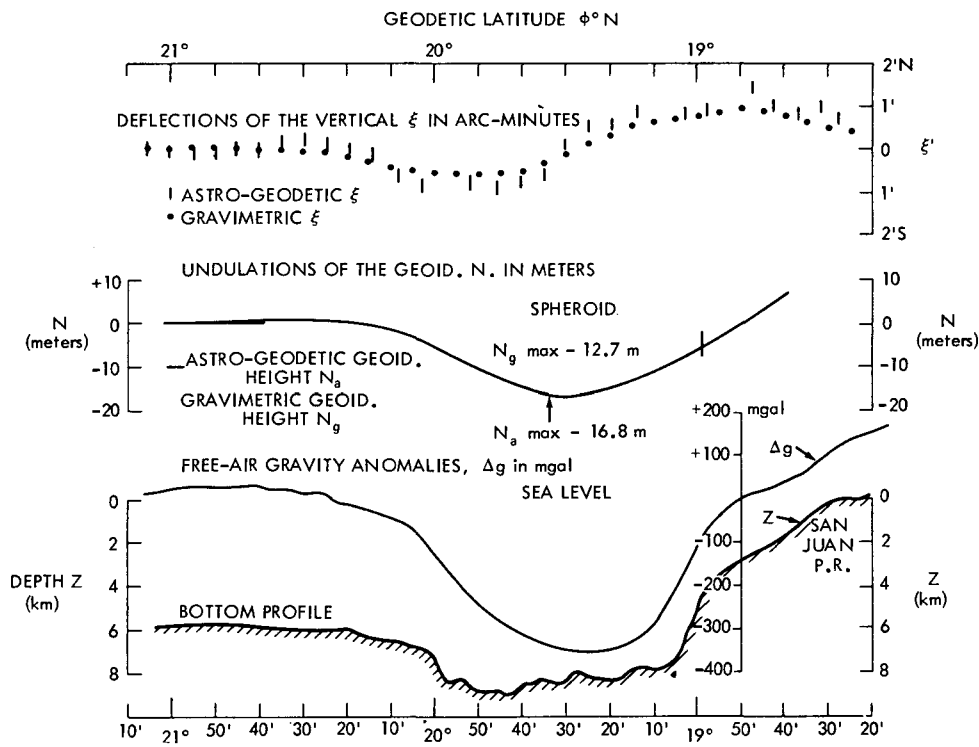
(From Level-Surface Profiles Across the Puerto Rico Trench,
W. Von Arx, Science, Vol. 154, No. 3757, December 1966)

Figure 5. Shape of the Geoid North of Puerto Rico.

B. Operational

The present method of sensing the gravity field of the sea surface using surface ships, submarines, and aircraft is limited in that only a small area of the sea surface can be covered at a given time. In fact, after years of making oceanographic measurements only 50% of the gravity field over the sea surface has been surveyed. A spacecraft-borne radar altimeter will be able to provide for the first time the capability of mapping the geoid in a short time frame (i.e., on the order of less than 1 year). In addition, with the increased accuracy of altimeters coupled with increased periods of operating the altimeter, the sensing of phenomena associated with the ocean dynamics will be possible.

III. EXPERIMENTAL APPROACH

A. Scientific Requirements:

In order to achieve the objective set forth in this experiment proposal, the following studies and corresponding analyses will be undertaken:

(a) Identification, analysis, and modelling of known error sources affecting the altimeter measurement. Error sources to be considered are:

    (1) Instrumental errors such as antenna offset, thermal noise, etc.
    (2) Propagation errors such as ionospheric and tropospheric refraction
    (3) Surface reflectivity
    (4) Synoptic effects such as winds, swells etc.
    (5) Tidal effects
    (6) Orbit errors due to the geopotential model, tracking system noise and bias; tracking system location, etc.

(b) Identification of undulation amplitudes and spectra of the known geoid. That is, in order to understand the geoidal undulations which are to be anticipated from the altimeter data, the vertical and horizontal scale of surface undulations from the best known models for the geoid will be identified.

(c) Development of mathematical models and computational algorithms required for processing altimeter data. Incorporation of the afore-mentioned computational algorithms into a geophysical research computer program which will be the analysis tool used for improving the models for the geopotential and the geoid.

(d) Application of the geophysical research computer program to perform simulation studies. These simulation studies will be used for:

    (1) Establishing tracking requirements necessary for achieving orbit accuracy needed for the reduction of altimeter data.
    (2) Establishing density of altimeter observations necessary for geopotential recovery.
    (3) Establishing the mathematical representation of the geopotential model most suitable for optimally utilizing altimetry data for describing the geopotential and geoid.

(e) Reduction and analysis of altimeter data for geopotential and geoid improvement.

B. <u>Mathematical Analysis</u>

A generalized description of a method for geopotential recovery using altimeter data is now to be discussed. The geometry for an instantaneous altitude measurement is shown in Figure 6. For illustrative purposes only, it is assumed that the altitude measurement is along the normal to the reference ellipsoid. A departure from the normal to the reference ellipsoid will be compensated for in the preprocessing of the altimeter data.

(a) Definitions:

$\vec{\rho}$: geocentric position vector of satellite

$\vec{R}$: geocentric position vector to subsatellite point on reference ellipsoid

$\vec{h}$: vector from subsatellite point on reference ellipsoid to satellite

h: magnitude of $\vec{h}$

h_g: geoidal height above reference ellipsoid

h_s: mean sea level height above geoid.

h_a: instantaneous height of satellite above sea levels (satellite altitude).

(b) Description of altimeter measurement.

From Figure 6.

$$\vec{h} = \vec{\rho} - \vec{R}$$

and

$$\vec{h}^0 = \frac{\vec{h}}{h} = \frac{\vec{\rho} - \vec{R}}{|\vec{\rho} - \vec{R}|}$$

then

$$\vec{h} = h\vec{h}^0 = (h_a + h_s + h_g)\vec{h}^0$$

$$h_a = (h - h_s - h_g)$$

13

ORBIT

MEAN SEA LEVEL

GEOID

SPHEROID
(reference ellipsoid)

h_a

h

$\vec{\rho}$

h_s

h_g

P

$\vec{R}$

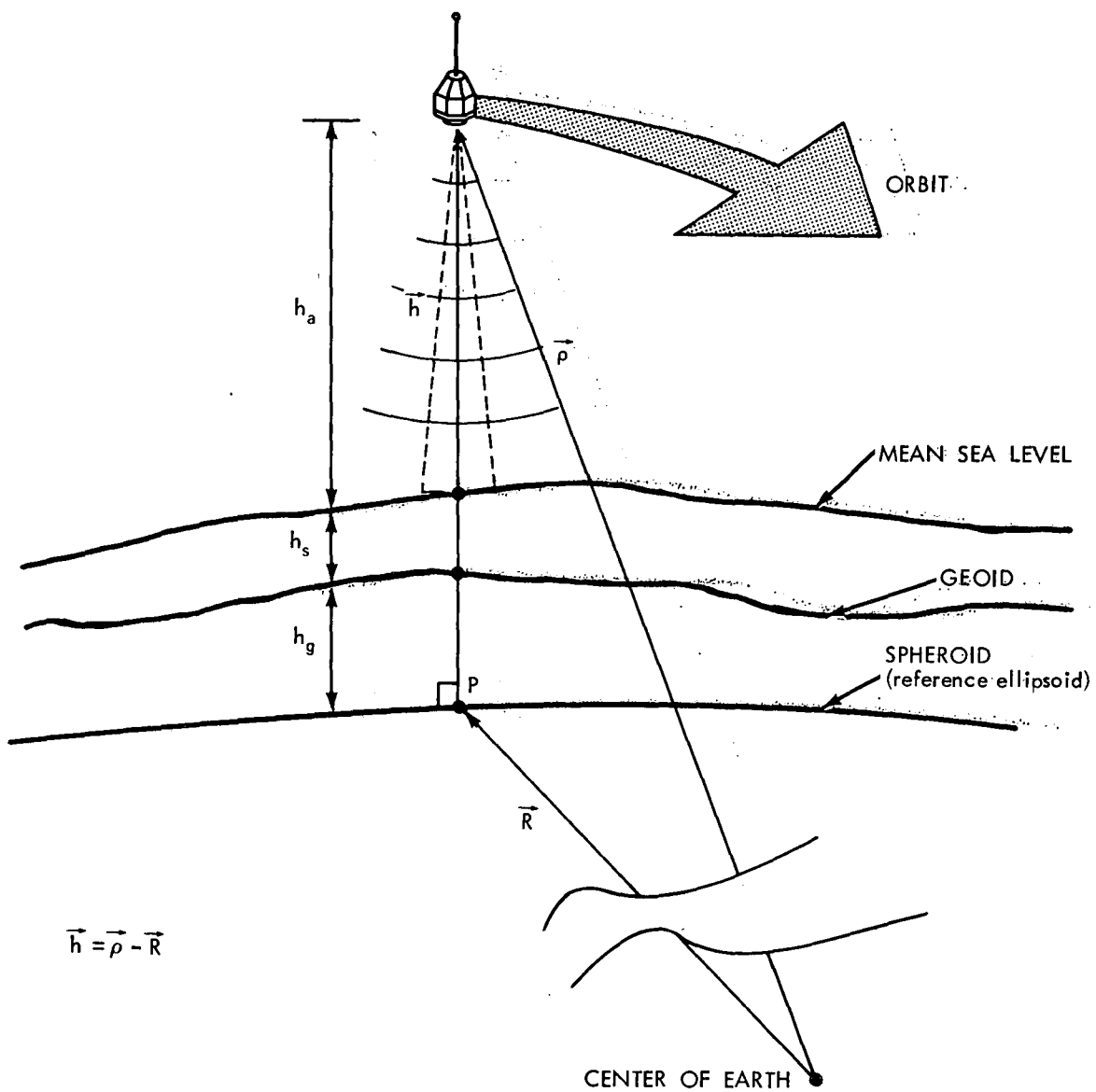$\vec{h} = \vec{\rho} - \vec{R}$

CENTER OF EARTH

Figure 6. Geometry for Instantaneous Altimeter Measurement.

The altitude measurement when written in functional form is therefore expressed as follows:

$$h_a = h_a \, (X, \, C_k, \, t)$$

(1.0)

where

X: state vector of satellite
i.e. $[x_1, \, x_2, \, x_3, \, \dot{x}_1, \, \dot{x}_2, \, \dot{x}_3]$

C_k: geopotential coefficients
i.e. $C_k = [C_{\ell m}, \, S_{\ell m}]$
$\ell \equiv$ degree index of harmonic coefficients
$m \equiv$ order index for harmonic coefficients

The geoidal height (h_g) is determined at each subsatellite point from the following equation:

$$h_g(\overline{\varphi}', \, \overline{\lambda}') = \frac{R_e^3}{4\pi\mu} \int_0^{2\pi} \int_{-\pi/2}^{\pi/2} \Delta g_T(\varphi', \, \lambda') \, S(\psi) \, \cos\varphi' \, d\varphi' \, d\lambda'$$

(2.0)

where

$S(\psi) \equiv$ Stokes' function
$= \csc(\psi/2) - 6\sin(\psi/2) + 1 - 5\cos(\psi)$
$- 3\cos(\psi)\log\{\sin(\psi/2) + \sin^2(\psi/2)\}$

$\psi = \cos^{-1}\{\sin\overline{\varphi}' \sin\varphi' + \cos\varphi'\cos\varphi' \cos(\overline{\lambda}' - \lambda')\}$

$(\overline{\varphi}', \, \overline{\lambda}')$: geocentric latitude and longitude of computational point for h_g.

$(\varphi', \, \lambda')$: geocentric latitude and longitude of variable integration point

$\Delta g_T \, (\varphi', \, \lambda')$: free air gravity anomaly at the variable point (φ', λ')

μ : product of universal gravity constant and mass of the earth

R_e : mean radius of the earth

e : ellipticity of reference ellipsoid.

$$\Delta g_T(\varphi', \lambda') =$$

$$\frac{\mu}{R_e^2} \sum_{\ell=2}^{k} \sum_{m-0}^{m} (\ell - 1) \left(\frac{R_e}{r}\right)^{\ell} P_{\ell m}(\sin \varphi') \{C_{nm} \cos m\lambda' + S_{nm} \sin m\lambda'\}$$

$$(3.0)$$

where

$k \equiv$ upper limit of degree and order of the geopotential model

$r \equiv$ geocentric radius

$$= (R + h_g) = \frac{R_e (1 - e^2)^{1/2}}{(1 - e^2 \cos^2 \varphi')^{1/2}} + h_g$$

The mean sea level height (h_s) will be obtained from observational data.

(c) Data Reduction and Analysis of Altimeter Measurements

Altimeter data will be corrected for known error sources, smoothed, sorted, etc. by the data preprocessor. Then, each "corrected" measurement h'_{a_i} will be compared with altitude calculated from the satellite's orbit. $(h'_{a_i})_\Omega$. Because of errors in the state, geopotential, etc.

$$h'_{a_i} \neq (h'_{a_i})_\Omega$$

and hence

$$\Delta \overline{h}' = h'_{a_i} - (h'_{a_i})_\Omega \neq 0$$

Using Equation (1.0), the error in h'_a is expressed as follows:

$$h'_a + \Delta \overline{h}' = h'_a (X + \Delta X, C_k + \Delta C_k, t) \qquad (4.0)$$

By expanding (4.0) in a Taylor's series one obtains the equation of condition relating the error in altitude to errors in the state and geopotential. That is,

$$\Delta \overline{h}'_c = \frac{\partial h'_a}{\partial X} \frac{\partial X}{\partial X_0} \Delta X_0 + \frac{\partial h'_a}{\partial (\Delta g)} \frac{\partial (\Delta g)}{\partial C_k} \Delta C_k + \epsilon \qquad (5.0)$$

16

where

$$\left(\frac{\partial X}{\partial X_0}\right)_{6 \times 6} \quad : \quad \text{State transition matrix}$$

$$\frac{\partial h'_{a_i}}{\partial (\Delta g)} : \quad \text{To be evaluated from (2.0)}$$

$$\frac{\partial (\Delta g)}{\partial C_k} : \quad \text{To be evaluated from (3.0)}$$

Letting

$$A_1 \equiv \frac{\partial h'_a}{\partial X} \frac{\partial X}{\partial X_0}$$

$$B_1 \equiv \frac{\partial h'_a}{\partial (\Delta g)} \frac{\partial (\Delta g)}{\partial C_k}$$

Then Equation 5.0 can be rewritten as follows:

$$\Delta \overline{h}'_c = A_1 \Delta X_0 + B_1 \Delta C_k + \epsilon \tag{5.1}$$

Measurements from ground tracking systems and from satellite to satellite tracking will be used to determine the orbit for the altimeter spacecraft. A generalized form for expressing these measurements (m_i) is as follows:

$$m_i = m_i(X, t) \tag{5.2}$$

The error in the measurement may then be expressed as

$$m_i + \Delta m_i = m_i(x + \Delta x, t) \tag{5.3}$$

(Here only the error in the state vector is considered as the major error source contributing to the error in the measurement m_i).

17

By expanding (5.3) in a Taylor's series, the condition equation for the ith measurement is:

$$\Delta m_i = \frac{\partial m_i}{\partial X} \frac{\partial X}{\partial X_0} \Delta X_0 + \overline{\epsilon}_i \qquad (5.4)$$

and the matrix equation representing all condition equations for other than altimeter measurements is written as follows:

$$\Delta m = A_2 \Delta X_0 + \epsilon \qquad (5.5)$$

where

$$A_2 \equiv \begin{bmatrix} \dfrac{\partial m_1}{\partial X} \dfrac{\partial X}{\partial X_0} \\ \cdot \\ \cdot \\ \cdot \\ \dfrac{\partial m}{\partial X} \dfrac{\partial X}{\partial X_0} \end{bmatrix}_{(p \times 6)}$$

and

$$\Delta m \equiv \begin{bmatrix} \Delta m_1 \\ \cdot \\ \cdot \\ \cdot \\ \cdot \\ \Delta m_p \end{bmatrix}_{(p \times 1)}$$

Altimeter measurements will be combined with other measurements to initially solve for corrections to the state vector in the least squares sense, i.e.

$$\Delta X_0 = [A_1^T W_1^{-1} A_1 + A_2^T W_2^{-1} A_2]^{-1} [A_1^T W_1^{-1} \Delta \overline{h}' + A_2^T W_2^{-1} \Delta m] \qquad (5.6)$$

were

W_1^{-1}: weighting matrix for altimeter measurements

W_2^{-1}: weighting matrix for other measurements used for orbit determination

18

After the kth iteration, "a best estimate" to the state vector of the satellite is determined.

That is

$$X_0^{(k)} = X_0^{(k-1)} + \Delta X_0^{(k)} \tag{5.7}$$

Now, by using only the altimeter data, a solution for estimating an improvement to both state and geopotential will be made using the estimate for state obtained from the kth iteration. That is, the solution of condition equations (5.1) for both state and geopotential gives the resultant correction to estimates for geopotential:

$$\Delta C_k = [(B_1^T B_1) - (B_1^T B_1) (A_1^T A_1)^{-1} (A_1^T B_1)]^{-1} [B_1^T \Delta \bar{h}' - (B_1^T A_1) (A_1^T A_1)^{-1} (A_1^T \Delta \bar{h}')]$$

and

$$C_k' = C_k + \Delta C_k \tag{5.8}$$

where

C_k' : the improved estimate for geopotential coefficients.

Likewise the new estimate to the state vector is:

$$X_0^{(k+1)} = X_0^{(k)} + \Delta X_0^{(k+1)}$$

The mathematical analysis described above considers the mathematical model used for the geopotential and geoid as a series expansion in spherical harmonics whose coefficients C_k are evaluated from the analysis of gravimetric, altimeter and tracking data, etc. Other models for geopotential exist, one example of such a model is one that expresses the geopotential in terms of surface density layers (Ref. 6). This model and others will be evaluated and tested for their possible application to geopotential recovery and geoid improvement using altimeter data.

C. Orbit Determination Requirements for the Altimeter Experiment

As part of the altimeter data reduction process, particularly over those regions where no tracking instrumentation exists, knowledge of the orbit for the spacecraft (s/c) is essential. The uncertainty in orbit altitude should be better than 1 meter. With this uncertainty in orbital altitude, variations of 5 meters and higher in the geopotential surface will be reflected in the resultant data residuals.

There should be no difficulty in attaining an uncertainty in orbital height to better than one meter since through the combination of surface tracking data and satellite to satellite tracking data for orbit determination almost complete tracking coverage of the orbit will be achieved. This type of coverage will minimize the effects of those orbital errors introduced by, for example, the geopotential model.

From the recent analysis of definitive orbits* for GEOS-II determined with C-Band radar range data and using the SAO-1969 Standard Earth model for the geopotential, it was consistently found that the total orbital uncertainty in GEOS II position ranged between 15 to 30 meters and the corresponding uncertainty in the radial component of the s/c position vector (equivalent to s/c height uncertainty) was found to range between ±5 meters.

Figure 7 shows the differences in height variation in the overlap region. That is, two, two-day orbital arcs each having a one-day data span period in common are compared.

The resultant variation in satellite height differences over this region has an absolute bound of approximately 5 meters and a rate of change of less than 50 cm/minute. Equating the rate of change in orbital height differences to the variation in orbital height uncertainty it is felt that, over the short periods that the altimeter measurements are made, the residuals resulting from the differencing between the measured and calculated orbital height should show variations of 5 meters or higher in geoidal height. Through the addition of satellite-to-satellite tracking, the additional tracking coverage should reduce the absolute uncertainty in orbital height to well below the 5 meter level. For example, Figure 8 shows the results of an error analysis study performed by Mr. J. Cooley in which it is shown that the error in orbital height for GEOS-C is in the one meter range when using satellite-to-satellite tracking. In this study the geosynchronous satellite ATS-F was placed at 94°W longitude, GEOS-C was assumed to be in a nominal 926 × 1204 km orbit with inclination 20°, and Rosman, North Carolina was assumed to be the ATS station with a position error of 10 meters in each coordinate (see Fig. 9).

Range and range rate tracking was simulated for a 24-hour period, with coverage by ATS-F limited to three 3-minute periods per GEOS-C pass at a sampling rate of 6 measurements/minute. A conservative range rate bias of 0.2 cm/sec was assumed for this study.

---

*The definitive orbit for GEOS II consisted of two-day orbital arcs with one-day overlap fitted to a 14-day span of data from 2/1/69 to 2/14/69.
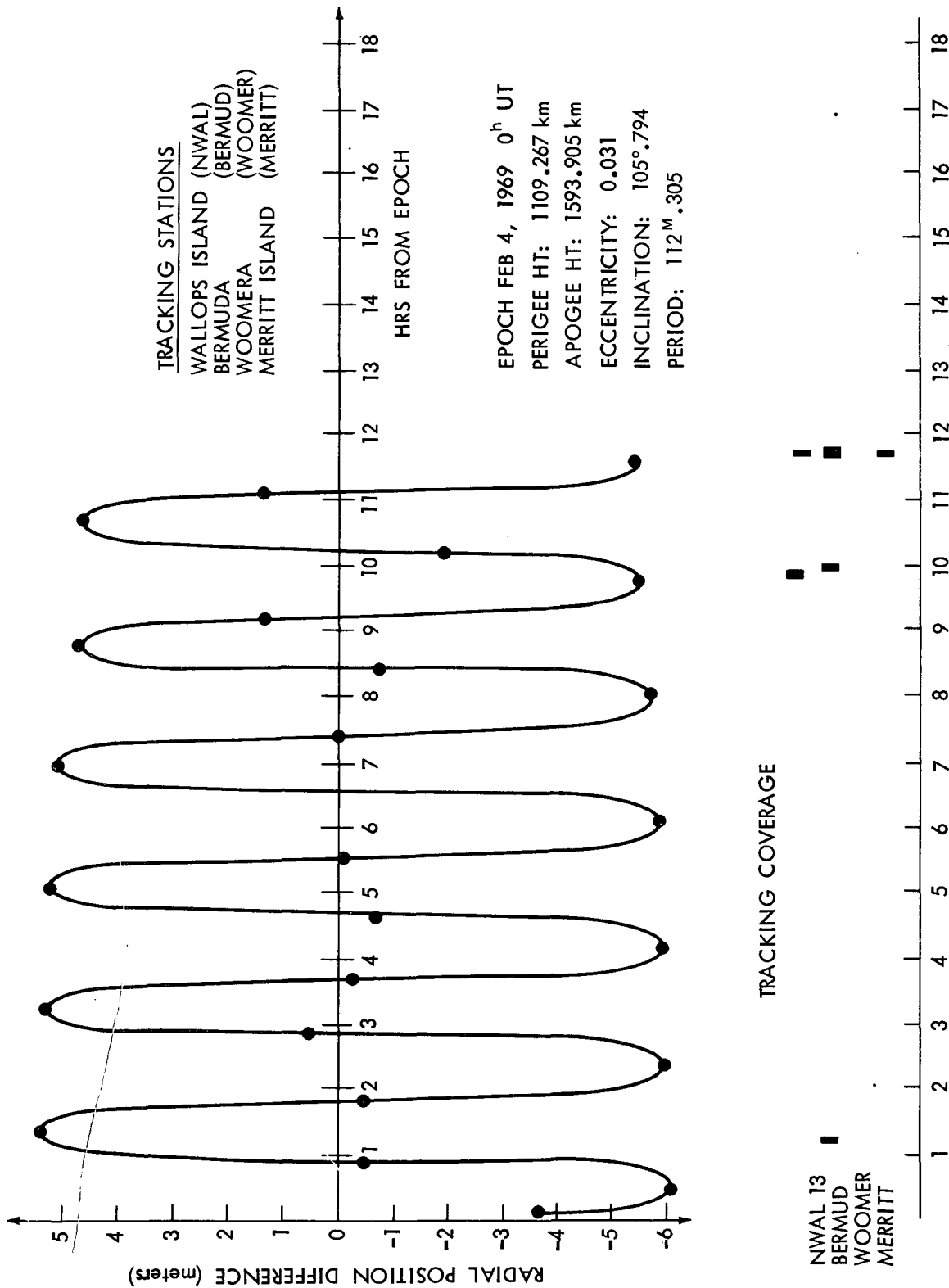
Figure 7. Differences in Radial Component of GEOS II Spacecraft Position Vector vs Time.

21

RANGE NOISE   = 3 m
RANGE BIAS   = 4 m
RANGE RATE NOISE = 1 cm/sec
RANGE RATE BIAS   = 0.2 cm/sec
A PRIORI (each coordinate)

	RANGE	RANGE RATE
ATS-F	288.684m	2cm/sec
GEOS-C	10m	0.05 cm/sec

Figure 8. ATS-F and GEOS-C Position Errors.

Figure 9. GEOS-C/ATS-F Link.

IV. SYSTEM DESCRIPTION

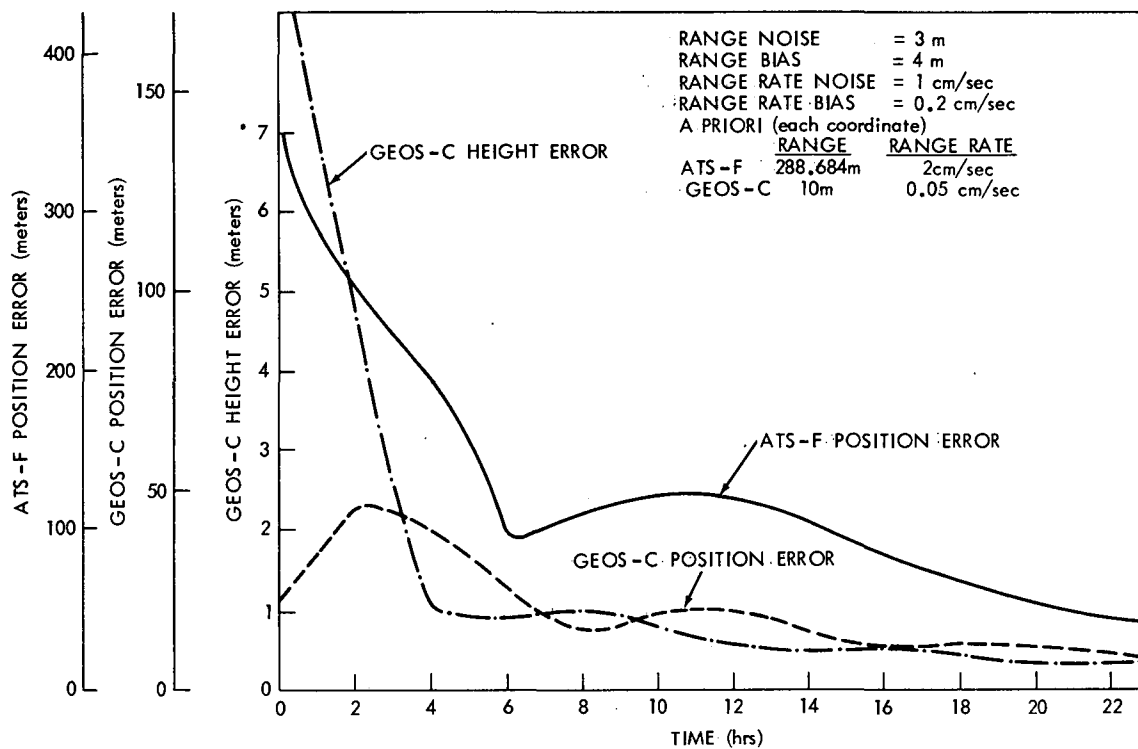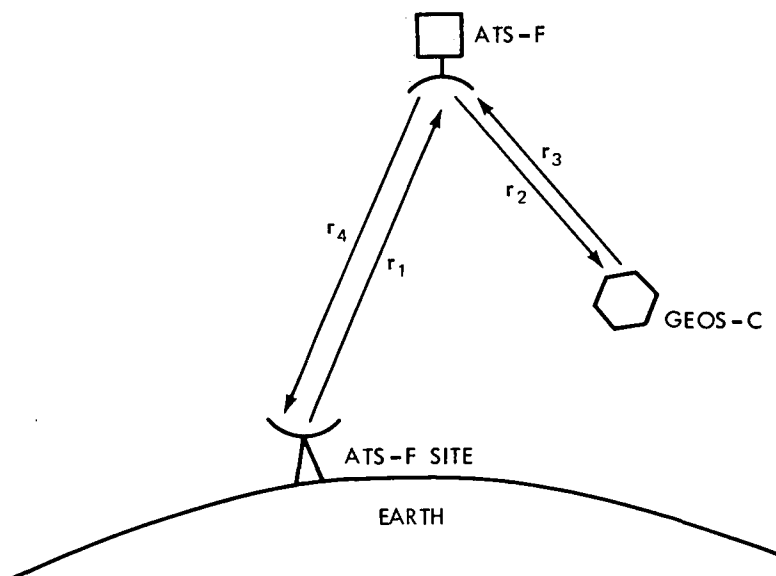A radar altimeter will be flown in a near circular orbit ($e \approx .0064$) with an inclination between 40° and 65° and a mean orbital altitude of approximately 1000 km (Reference 7). Altimeter data will be transmitted via the telemetry subsystem in real time when the spacecraft will be within the range of ground tracking systems capable of receiving telemetry (TM) data and will be stored in a memory for delayed readout, when the spacecraft is over areas outside the range of tracking/TM facilities. The detailed description of the radar altimeter instrumental package will be found in the GEOS-C altimeter technical plan (Reference 7), and evaluation. A system error analysis will be performed using observational data obtained during the experiment.

A. Description of Principal Error Sources

The errors in the altitude measurements are categorized as instrumental errors, propagation errors, and as reflecting surface anomalies. Each of these error sources is further delineated as a bias (an error source which tends to increase or decrease a measurement by a fixed amount) and random noise (those errors for which it is impossible to predict the precise final state of the phenomenon from the initial state and the known laws of nature).

Some of the error sources which are to be evaluated for the altimeter experiment are the following:

1. Instrumental Error

This error is the sum of those instrumental errors which are independent of signal strength, surface reflectivity, path anomalies, altitude rate, and attitude angle. These errors may be a function of instrument temperature, voltage regulation, clock stability, or instrument aging, and may be bias or noise type.

Thermal Noise

This error is the result of noise (internally and externally generated) entering the tracking electronics and causing either a fixed offset or a random jitter in the altitude reading. For large signal-to-noise ratios, this can be ignored. The value of SNR beyond which this error can be ignored will be derived from the tracking loop and data sampling design.

Propagation Errors

These errors in the altitude are caused by the radio frequency signal propagating through the ionosphere and the troposphere. The error due to the ionosphere is considered much less than a centimeter even for a disturbed ionosphere (Ref. 10). Mr. Gordon Thayer of the National Bureau of Standards as cited by T. Godbey (Ref. 11) gives a mean altitude error for the troposphere of 2.6 meters which is resolvable to ±3 centimeters using ground based radar soundings. A regression analysis of the altimeter data coupled with orbital tracking systems (i.e., C-band radars and lasers) data should further resolve this error.

Other propagation path anomalies include cloud and rain attenuation effects. Data extracted from Barton, Figure 15.4 (Ref. 10) indicates that these effects will only alter the altitude accuracy during heavy rain storms coupled with low SNR. While these effects will not be excluded from the evaluation, they will be treated only as a special case if the proper sequence of meteorological events occur.

Surface Reflectivity Error

This is perhaps the prime error to be evaluated from the data. The sea surface is a random distribution of energy scatterers. As such the location of the apparent reflecting surface is not clearly defined. This lack of definition is compounded by the variable sea state that may exist from one altimeter pass to another (References 12, 20, 21, 22). In order to evaluate this quantity and categorize the data, it will be necessary to obtain actual sea conditions at the time of the pass in the illuminated area. This information should be obtainable from the Naval Oceanographic Office or an office of Marine Studies (contacts for obtaining this data will be made when approval of this proposal is received).

5. Altitude Rate Errors

The altimeter will not incorporate an acceleration tracking loop and thus will have a dynamic velocity lag. The error voltage developed by the servo must be recorded and present in the data in order that this lag can be evaluated. Prelaunch simulation will establish an approximation of this lag. However, the exact effect of the surface reflectivity upon this error must be evaluated in orbit.

6. Attitude Angle Errors

This error is the result of the return pulse being distorted by the antenna not looking perpendicular to the surface of the ocean. The analysis will establish the exact bias value versus angle off nadir. A data readout of angle off nadir is required to verify this bias value.

B. Evaluation Procedures for Error Sources

Procedures are discussed and categorized for evaluating the principal error sources which influence the performance of the radar altimeter. These procedures are outlined in accordance with the error sources identified above:

1. Static Instrumental Error

To perform a system evaluation, the instrumental errors attributable to the altimeter, detail circuit analysis of the tracking loop, time discriminator, clock frequency and clock long term and short term stability, transmitted pulse shape as a function of time within the pulse (pulse compression mode as well as conventional model), pulse repetition frequency, receiving system noise temperature, automatic gain control characteristics, and detector functional characteristics must be known.

The above information can be obtained during preflight testing and calibration or may be supplied by the manufacturer as a result of internal qualification tests. A detailed evaluation of the instrumental error is a required input for this experiment.

2. Surface Reflectivity Error

The requirements which must be met for analyzing this error source requires that the altimeter be operated over water and that surface vessels be available to actually record the surface characteristics within one (1) hour before or after the operational pass. The operational pass can be either daylight or night, however, there must be sufficient ambient surface light for visual sea characteristics observations. An ideal situation for this test is in an area where extensive ground track of the spacecraft is available.

3. Thermal Noise

This quantity is readily available in an approximate form from the automatic gain control (agc) voltage of the system receiver. The agc voltage as read from the receiver is a measure of the received signal plus noise. The ratio of signal plus noise to noise can then be determined from the system noise temperature.

4. Propagation Errors

Ideal test conditions for this evaluation will be at least two passes during clear weather plus at least two passes during rain or cloudy weather. Meteorological data should be available on moisture content cloud density, and cloud

thickness in the path of the propagating r.f. energy. Radar sounding data of the troposphere will be requested from the National Bureau of Standards.

5. Altitude Rate Error

This error source will be evaluated by comparing the altitude rate computed from the orbit with the measured altitude rate. The tracking loop error voltage is required to evaluate the velocity errors.

6. Attitude Angle Error

The antenna should point at the nadir. If antenna pointing deviates from the nadir, the angle between the nadir and antenna bore site should be available with a precision of at least 1/4 of the antenna bandwidth.

C. Data Requirements

For the evaluation of radar altimeter data as well as application of these data to geopotential recovery and improvement of the global geoid, accuracy, data logs and tapes consisting of the following are required:

1. Instrumental Data consisting of:

    (a) Functional design of receiver, time discriminator, and tracking loop.

    (b) Clock frequency and stability.

    (c) Transmitter pulse shape (pulse compression and conventional modes).

    (d) Pulse repetition frequency.

    (e) Receiving System noise temperature.

    (f) Automatic gain control characteristics.

    (g) Receiver detection system.

    (h) Antenna patterns (45° cuts).

    (i) Sampling gate widths.

    (j) Sampling gate positions.

    (k) Sampling gate width and positional accuracy.

    (l) Instrument temperature.

    (m) Transmitter power.

    (n) Receiver delay or altitude zero set versus temperature and voltage.

2. Test Data consisting of:

    (a) Indicated altitude or propagation delay.

    (b) All return pulse samples.

    (c) Time correlated data of altitude and pulse samples.

    (d) Sea state (surface observation).

    (e) Wave Height (surface observation).

    (f) Surface wind (surface observation).

    (g) Altitude servo error voltage.

    (h) Antenna angle vs. nadir.

    (i) Meteorological conditions above altimeter test areas.

    (j) Orbital altitude determined by ground tracking systems over altimeter test sites

References

1. NASA CR 1579 "The Terrestrial Environment: Solid-Earth and Ocean Physics," Washington, D. C., April 1970.

2. Vonbun, F. O., "Geodetic Satellite Mission and Spacecraft," NASA/GSFC XIII Plenary Meeting of COSPAR, May 1970.

3. Hudson, E. F., "A Geodetic and Oceanographic Satellite Altimeter System," AIAA Paper No. 71-845, July 1971.

4. Strange, W. E. et. al., "A Detailed Gravimetric Geoid for the United States;" NASA/GSFC X-Report, X-552-71-219; June 1971.

5. Von Arx, W. S., "Level-Surface Profiles Across the Puerto Rico Trench," SCIENCE, Vol. 154, pp. 1651-1653, Dec. 30, 1966.

6. Koch, K. R., and Witte, B. U., "The Earth's Gravity Field Represented by a Simple Layer Potential From Doppler Tracking of Satellites," NOAA Technical Memorandum NOS 9, April 1971.

7. "Project Plan for Geodetic Orbiting Satellite (GEOS-C) – Phases C&D Combined – Preliminary unpublished 1971.

8. Vonbun, F. O., Memorandum "Calibration of the Radar Altimeter for GEOS-C," Feb. 4, 1970.

9. "GEOS-C Radar Altimeter System Technical Plan," Wallops Island, October, 1970.

10. Barton, D. K., "Radar System Analysis," Prentice-Hall, Oct. 1965.

11. Godbey, T. W., "Oceanographic Satellite Radar Altimeter and Wind Sea Sensor," Proceedings of Conf. on the Feasibility of Oceanographic Explorations from Aircraft, Aug. 1964.

12. Bryan, J. W., "Satellite Altimetry," NASA/GSFC X-Report X-551-70-248, June 1970.

13. Pearson, W. J., Mear, E., "The Effects of Wind Waves and Swell on the Ranging Accuracy of a Radar Altimeter (Part 1)," Report prepared for U.S. Naval Oceanographic Office – Contract N62306-70-A-0075, Jan. 1970.

14. Greenwood, J. A., et. al., "Radar Altimetry from a Spacecraft and Its Potential Applications to Geodesy," Remote Sensing of Environment 1 (1969), pp. 59-70.

15. Greenwood, J. A., et. al., "Oceanographic Applications of Radar Altimeter from a Spacecraft," Remote Sensing of Environment 1 (1969), pp. 71-80.

16. Lundquist, C. A., "Satellite Altimetry and Orbit Determination," SAO Special Report 248, August 1967.

17. Lundquist, C. A., Giacaglia, G.E.O., et. al., "Possible Geopotential Improvement from Satellite Altimetry," SAO Special Report, Feb. 1969.

18. Gaposchkin, E. M., Lanbeck, K., "1969 Smithsonian Standard Earth," SAO Special Report 315, May 1970.

19. Raytheon, "Space Geodesy Altimeter Study," Final Report, NASW1790, Oct. 1968.

20. Skolnik, M., "A Review of Radar Sea Echo," NRL Report 2025, July 1969.

21. Moore, P. K. and Bradley, G., "Radar and Oceanography," Microwave Observation of the Ocean, June 1969.

22. Wright, J. W., "A New Model for Sea Clutter," IEE Trans. on Antennas and Propagation, March 1968, pp. 217-223.